Int. J. Solids Structures Vol. 29, No. 12, pp. 1581–1595, 1992
Printed in Great Britain.

0020-7683/92 $5.00+.00

EFFECTIVE LONGITUDINAL SHEAR MODULUS OF A UNIDIRECTIONAL FIBER COMPOSITE CONTAINING INTERFACIAL CRACKS

HONG TENG
Department of Theoretical and Applied Mechanics, University of Illinois at Urbana-Champaign, Urbana, IL 61801, U.S.A.

(Received 12 February 1991; in revised form 30 September 1991)

Abstract—The problem of evaluating the effective longitudinal shear modulus of a unidirectional fiber composite containing fiber-matrix interfacial cracks is considered. The generalized self-consistent scheme is employed in the formulation of the problem. The resulting mixed boundary value problem leads to a system of dual series equations, which can then be reduced to Fredholm integral equations of the first kind with a logarithmically singular kernel. The reduced longitudinal shear modulus is calculated by solving the governing weakly singular integral equations.

INTRODUCTION

The presence of many cracks in a composite material may cause reduction in its stiffness, thus degrading the integrity of the material.

The problem of analysing stiffness reduction due to the presence of cracks, like other crack problems for composite materials, may be attacked by two fundamentally different approaches. One is the macromechanics approach that approximates heterogeneous composite materials as homogeneous but anisotropic media. The other is the micromechanics approach which inevitably leads to the treatment of cracks in dissimilar materials. A large number of solutions exist in the technical literature for dissimilar materials containing cracks of various locations and orientations. As it is well recognized that cracks are more likely to develop at interfaces between two different constituent materials of a composite medium, a considerable amount of work has been devoted to the analysis of interfacial cracks [see Comninou (1990) for review and further references]. However, most of the investigations were concerned with cracks near or at an interface of two semi-infinite media rendering no direct applications to the problem of stiffness reduction caused by interface cracks present in composite materials.

Although a number of studies has been made on the evaluation of effective elastic moduli of cracked homogeneous materials [for instance, Delameter *et al.* (1975), Hoenig (1979)], the work on cracked fiber composites in the light of micromechanics analysis is still relatively rare in the literature. Highly approximate treatments of the reduction in longitudinal Young's modulus of an aligned short-fiber reinforced composite weakened by fiber-end cracks and a unidirectional fiber composite with broken fibers were given by Takao *et al.* (1982) and Steif (1984), respectively, in which the singular nature of the stress field in the vicinity of a crack has not been taken into account. The problem of calculating elastic moduli of unidirectional fiber composites containing matrix cracks was considered by Laws *et al.* (1983).

To permit a comparatively simple analytical formulation, in the present paper we consider the problem of evaluating the reduced longitudinal shear modulus of a unidirectional fiber composite containing interfacial cracks. The generalized self-consistent scheme is employed to evaluate the effective shear modulus of the composite weakened by those cracks. This method has been applied by Christensen and Lo (1979) to calculate elastic moduli of fiber-reinforced composites with perfect interface, and later extended to imperfect interface conditions (Hashin, 1990). The self-consistent analysis has also been applied rather frequently to calculate elastic moduli of cracked homogeneous materials. In the two-dimensional crack configuration of the present problem, cracks are assumed to take place along the entire length of the fiber, which may not happen in general. The resulting mixed boundary value problem leads to a system of dual series equations, which can then be reduced to Fredholm integral equations of the first kind with a logarithmically singular kernel. Although great difficulty is generally to be expected in numerically solving Fredholm integral equations of the first kind with a smooth kernel, the presence of the logarithmic singularity in the current problem makes the integral equations amenable to numerical solution. The reduced longitudinal shear modulus is then calculated by solving the governing weakly singular integral equations.

Problems related to fiber-reinforced composites under longitudinal shearing have been studied by many authors (Adams and Doner, 1967; Budiansky and Carrier, 1984; Steif and Dollar, 1988). The dual series approach adopted in this paper has been used in solving various mixed boundary value problems such as the separation of an inclusion from an infinite matrix (Keer *et al.*, 1973) and the bending of cracked beams (Westmann and Yang, 1967) and plates (Keer and Sve, 1970).

FORMULATION OF THE PROBLEM

Consider a unidirectional fiber-reinforced composite as shown in Fig. 1 with some of the fibers containing interfacial cracks. Both the fibers and the matrix are taken to be homogeneous, isotropic and linearly elastic, with shear modulus of G_f and G_m, respectively. It is assumed that the interface cracks are randomly located so that the composite material remains transversely isotropic. It is further assumed that fibers contain only single cracks, but the crack size may vary from fiber to fiber. As illustrated in Fig. 2, the location of the crack at the fiber–matrix interface is defined by the angle β, and the extent of the crack is measured by the angle α with the half crack length $c = \alpha a$, where a is the fiber radius.

To determine the effective longitudinal shear modulus G_e, a longitudinal shear stress $\tau_{23} = \tau_0$ is applied to the composite material as illustrated in Fig. 1. The problelm is that of the anti-plane strain deformation, and the only nonvanishing displacement is the longitudinal component w. It follows that

$$G_e = \frac{\bar{\tau}_{23}}{2\bar{\varepsilon}_{23}} \tag{1}$$

where $\bar{\tau}_{23}$ and $\bar{\varepsilon}_{23}$ are respectively the average stress and strain in the composite. Using the average stress theorem, it can be shown that $\bar{\tau}_{23} = \tau_0$. Applying the average strain theorem, $\bar{\varepsilon}_{23}$ can be expressed in terms of the fiber and matrix strain averages $\bar{\varepsilon}^f_{23}$ and $\bar{\varepsilon}^m_{23}$, respectively, and the displacement jump $[w]$ across the interface cracks as

$$2\bar{\varepsilon}_{23} = 2V_f\bar{\varepsilon}^f_{23} + 2(1-V_f)\bar{\varepsilon}^m_{23} + \Gamma_{23} \tag{2}$$

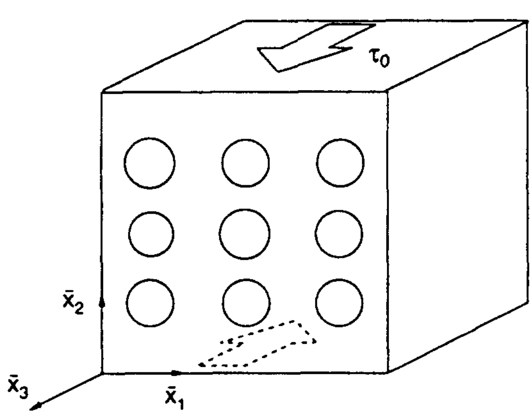

Fig. 1. Longitudinal shearing of a unidirectional fiber composite.

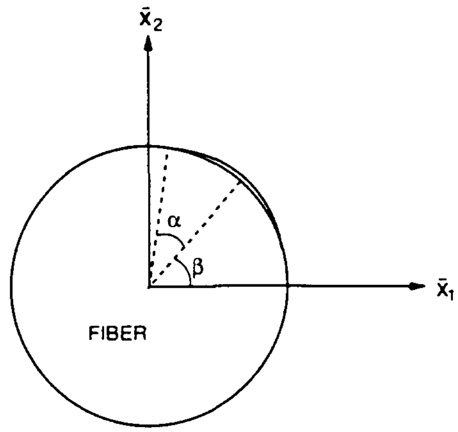

Fig. 2. Crack configuration.

with

$$\Gamma_{23} = \frac{1}{A}\int_{S_c} [w] n_2 \, \mathrm{d}s \tag{3}$$

where V_f is the fiber volume fraction, A is the composite specimen cross-section area, S_c denotes the contour of all the cracked interfaces, n_2 denotes the x_2-component of the outward normal of the contour and $\mathrm{d}s$ is the element of arc length of the contour. Using the stress–strain relations for the fiber and the matrix materials and eliminating the matrix average stress one finds that

$$2\bar{\varepsilon}_{23} = V_f\left(\frac{1}{G_f} - \frac{1}{G_m}\right)\bar{\tau}^f_{23} + \frac{\bar{\tau}_{23}}{G_m} + \Gamma_{23} \tag{4}$$

and it follows from (1) that

$$\frac{G_m}{G_c} = 1 + V_f\left(\frac{G_m}{G_f} - 1\right)\frac{\bar{\tau}^f_{23}}{\tau_0} + \frac{G_m}{\tau_0}\Gamma_{23}. \tag{5}$$

Equation (5) constitutes the basic equation for calculating the effective longitudinal shear modulus of the fiber composite containing interfacial cracks under consideration. Evaluation of the average fiber stress and the interface displacement integral in (5) is done by utilizing the generalized self-consistent scheme. The underlying assumption of the generalized self-consistent scheme in the present context is that the average state of stress and strain in any individual fiber is estimated by embedding a composite cylinder, consisting of a fiber with radius a and a concentric matrix shell with radius b such that the fiber volume content in the composite cylinder is the same as the gross composite material, in an infinite homogeneous and transversely isotropic material having the effective longitudinal shear modulus G_c yet to be determined, and a longitudinal shear stress τ_0 is applied at infinity.

We introduce local crack coordinates (x_1, x_2, x_3) as opposed to the global coordinates $(\bar{x}_1, \bar{x}_2, \bar{x}_3)$ with $x_3 = \bar{x}_3$, along with the corresponding polar coordinates (r, θ). It is defined

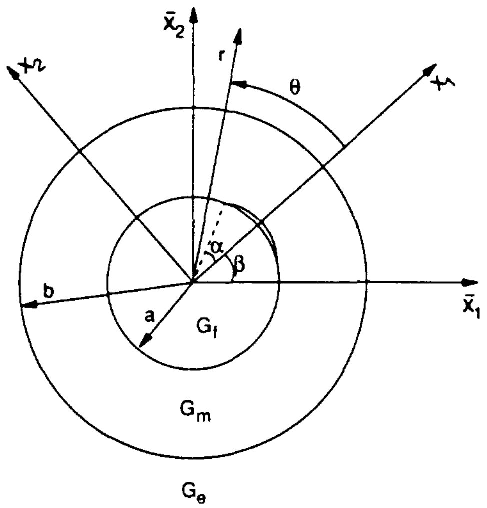

Fig. 3. Generalized self-consistent scheme model.

with respect to a single crack as illustrated in Fig. 3 with the x_1-axis passing through the center of the crack arc. It is convenient to consider the problem in the local polar coordinate system. Hence a three-phase boundary value problem needs to be solved to obtain the average fiber stress and the interface displacement integral in (5). Since the average is taken over all the fibers and the integral over all the cracked interfaces, this boundary value problem has to be solved many times according to cracks with different sizes. Since the yet unknown effective modulus G_e enters the solution itself of the three-phase self-consistent model, an iterative procedure is apparently required to solve (5) for G_e.

The displacement function $w(r,\theta)$ is harmonic, satisfying Laplace's equation

$$\nabla^2 w = 0 \tag{6}$$

with corresponding shear stress components given by

$$\tau_{rz} = G\frac{\partial w}{\partial r}, \quad \tau_{\theta z} = G\frac{1}{r}\frac{\partial w}{\partial \theta} \tag{7}$$

where G denotes the shear modulus. The above expressions are valid for the fiber, the matrix and the effective material provided that G is replaced by G_f, G_m and G_e respectively. The following boundary condition at infinity is obtained with reference to the local polar coordinates

$$\tau_{rz} = \tau_0 \cos\beta \sin\theta + \tau_0 \sin\beta \cos\theta, \quad r \to \infty. \tag{8}$$

The solution to Laplace's equation (6) is expressed as $w(r,\theta) = w^{(1)}(r,\theta) + w^{(2)}(r,\theta)$, where $w^{(s)}(r,\theta), s = 1,2$, are odd and even functions of θ, respectively. The corresponding stress components can be written as $\tau_{rz}r,\theta) = \tau_{rz}^{(1)}(r,\theta) + \tau_{rz}^{(2)}(r,\theta)$, $\tau_{\theta z}(r,\theta) = \tau_{\theta z}^{(1)}(r,\theta) + \tau_{\theta z}^{(2)}(r,\theta)$. Denoting the solutions in the three regions of $0 < r < a$, $a < r < b$ and $r > b$ by superscripts f, m and e respectively, we have

$$w^{(1)f} = \sum_{n=1}^{\infty} A_n^{(1)} r^n \sin n\theta \tag{9}$$

$$w^{(1)m} = \sum_{n=1}^{\infty} \left(B_n^{(1)} r^n + \frac{C_n^{(1)}}{r^n} \right) \sin n\theta \tag{10}$$

$$w^{(1)\mathrm{c}} = \sum_{n=1}^{\infty} \frac{D_n^{(1)}}{r^n} \sin n\theta + \frac{\tau_0 \cos \beta}{G_\mathrm{c}} r \sin \theta \tag{11}$$

and

$$w^{(2)\mathrm{f}} = \sum_{n=0}^{\infty} A_n^{(2)} r^n \cos n\theta \tag{12}$$

$$w^{(2)\mathrm{m}} = \sum_{n=1}^{\infty} \left(B_n^{(2)} r^n + \frac{C_n^{(2)}}{r^n} \right) \cos n\theta \tag{13}$$

$$w^{(2)\mathrm{c}} = \sum_{n=1}^{\infty} \frac{D_n^{(2)}}{r^n} \cos n\theta + \frac{\tau_0 \sin \beta}{G_\mathrm{c}} r \cos \theta. \tag{14}$$

Due to the symmetries, only the region of $0 \leqslant \theta \leqslant \pi$ need be considered.

By using (7), the radial shear stress components can be expressed as

$$\tau_{rz}^{(1)\mathrm{f}} = G_\mathrm{f} \sum_{n=1}^{\infty} n A_n^{(1)} r^{n-1} \sin n\theta \tag{15}$$

$$\tau_{rz}^{(1)\mathrm{m}} = G_\mathrm{m} \sum_{n=1}^{\infty} n \left(B_n^{(1)} r^{n-1} - \frac{C_n^{(1)}}{r^{n+1}} \right) \sin n\theta \tag{16}$$

$$\tau_{rz}^{(1)\mathrm{c}} = G_\mathrm{c} \sum_{n=1}^{\infty} -n \frac{D_n^{(1)}}{r^{n+1}} \sin n\theta + \tau_0 \cos \beta \sin \theta \tag{17}$$

and

$$\tau_{rz}^{(2)\mathrm{f}} = G_\mathrm{f} \sum_{n=1}^{\infty} n A_n^{(2)} r^{n-1} \cos n\theta \tag{18}$$

$$\tau_{rz}^{(2)\mathrm{m}} = G_\mathrm{m} \sum_{n=1}^{\infty} n \left(B_n^{(2)} r^{n-1} - \frac{C_n^{(2)}}{r^{n+1}} \right) \cos n\theta \tag{19}$$

$$\tau_{rz}^{(2)\mathrm{c}} = G_\mathrm{c} \sum_{n=1}^{\infty} -n \frac{D_n^{(2)}}{r^{n+1}} \cos n\theta + \tau_0 \sin \beta \cos \theta. \tag{20}$$

Similar expressions may be written for the corresponding tangential shear stress components.

The solutions are required to satisfy the boundary conditions at $r = a$

$$\tau_{rz}^{(s)\mathrm{f}}(a, \theta) = \tau_{rz}^{(s)\mathrm{m}}(a, \theta), \quad \alpha \leqslant \theta \leqslant \pi \tag{21}$$

$$\tau_{rz}^{(s)\mathrm{f}}(a, \theta) = \tau_{rz}^{(s)\mathrm{m}}(a, \theta) = 0, \quad 0 \leqslant \theta \leqslant \alpha \tag{22}$$

$$w^{(s)\mathrm{f}}(a, \theta) = w^{(s)\mathrm{m}}(a, \theta), \quad \alpha \leqslant \theta \leqslant \pi \tag{23}$$

and the boundary conditions at $r = b$

$$\tau_{rz}^{(s)\mathrm{m}}(b, \theta) = \tau_{rz}^{(s)\mathrm{c}}(b, \theta), \quad 0 \leqslant \theta \leqslant \pi \tag{24}$$

$$w^{(s)m}(b,\theta) = w^{(s)c}(b,\theta), \quad 0 \leqslant \theta \leqslant \pi \tag{25}$$

$$s = 1, 2.$$

The boundary conditions are mixed, and they lead to the following dual series equations

$$\sum_{n=1}^{\infty} na^{n-1}A_n^{(1)} \sin n\theta = 0, \quad 0 \leqslant \theta \leqslant \alpha \tag{26}$$

$$\sum_{n=1}^{\infty} (1+\beta_n)a^n A_n^{(1)} \sin n\theta = F_1(\theta), \quad \alpha \leqslant \theta \leqslant \pi \tag{27}$$

and

$$\sum_{n=1}^{\infty} na^{n-1}A_n^{(2)} \cos n\theta = 0, \quad 0 \leqslant \theta \leqslant \alpha \tag{28}$$

$$A_0^{(2)} + \sum_{n=1}^{\infty} (1+B_n)a^n A_n^{(2)} \cos n\theta = F_2(\theta), \quad \alpha \leqslant \theta \leqslant \pi \tag{29}$$

where

$$\lambda = \frac{G_f}{G_m} \tag{30}$$

$$\bar{G} = \frac{G_c}{G_m} \tag{31}$$

$$\beta_n = \lambda \frac{1+\bar{G}+(1-\bar{G})V_f^n}{1+\bar{G}-(1-\bar{G})V_f^n} \tag{32}$$

$$F_1(\theta) = \frac{4}{1+\bar{G}-(1-\bar{G})V_f} \frac{\tau_0 \cos \beta}{G_m} a \sin \theta \tag{33}$$

$$F_2(\theta) = \frac{4}{1+\bar{G}-(1-\bar{G})V_f} \frac{\tau_0 \sin \beta}{G_m} a \cos \theta. \tag{34}$$

SOLUTIONS OF THE DUAL SERIES EQUATIONS

We now proceed to construct the solutions for the dual series equations (26)–(27) and (28)-(29). For this purpose, let $H_1(\theta)$ and $H_2(\theta)$ denote the anti-symmetric and symmetric parts of the shear traction along the uncracked portion of the interface. It follows that

$$G_f \sum_{n=1}^{\infty} na^{n-1}A_n^{(1)} \sin n\theta = \begin{cases} H_1(\theta), & \alpha \leqslant \theta \leqslant \pi \\ 0, & 0 \leqslant \theta < \alpha \end{cases} \tag{35}$$

$$G_f \sum_{n=1}^{\infty} na^{n-1}A_n^{(2)} \cos n\theta = \begin{cases} H_2(\theta), & \alpha \leqslant \theta \leqslant \pi \\ 0, & 0 \leqslant \theta < \alpha. \end{cases} \tag{36}$$

The Fourier coefficients $A_n^{(1)}$ and $A_n^{(2)}$ are given by

$$A_n^{(1)} = \frac{2}{\pi G_f n a^{n-1}} \int_\alpha^\pi H_1(\phi) \sin n\phi \, \mathrm{d}\phi \tag{37}$$

$$A_n^{(2)} = \frac{2}{\pi G_f n a^{n-1}} \int_\alpha^\pi H_2(\phi) \cos n\phi \, \mathrm{d}\phi \tag{38}$$

$$n = 1, 2, 3, \ldots$$

and

$$\int_\alpha^\pi H_2(\phi) \, \mathrm{d}\phi = 0. \tag{39}$$

Substituting (37) and (38) into (27) and (29), respectively, and changing the order of integration and summation, we arrive at the following Fredholm integral equations of the first kind

$$\int_\alpha^\pi \bar{H}_1(\phi) K_1(\theta, \phi) \, \mathrm{d}\phi = f_1(\theta) \tag{40}$$

$$\frac{G_m}{2a\tau_0 \sin\beta} A_0^{(2)} + \int_\alpha^\pi \bar{H}_2(\phi) K_2(\theta, \phi) \, \mathrm{d}\phi = f_2(\theta) \tag{41}$$

where $H_1(\phi) = \pi\lambda \bar{H}_1(\phi)\tau_0 \cos\beta$, $H_2(\phi) = \pi\lambda \bar{H}_2(\phi)\tau_0 \sin\beta$ and

$$\int_\alpha^\pi \bar{H}_2(\phi) \, \mathrm{d}\phi = 0 \tag{42}$$

$$K_1(\theta, \phi) = \sum_{n=1}^{\infty} (1+\beta_n) \frac{1}{n} \sin n\theta \sin n\phi \tag{43}$$

$$K_2(\theta, \phi) = \sum_{n=1}^{\infty} (1+\beta_n) \frac{1}{n} \cos n\theta \cos n\phi \tag{44}$$

$$f_1(\theta) = \frac{2}{1+\bar{G}-(1-\bar{G})V_f} \sin\theta \tag{45}$$

$$f_2(\theta) = \frac{2}{1+\bar{G}-(1-\bar{G})V_f} \cos\theta. \tag{46}$$

The kernels of the integral equations (40) and (41) contain a logarithmic singularity. To see this, let (43) and (44) be rewritten as

$$K_1(\theta, \phi) = (1+\lambda) \sum_{n=1}^{\infty} \frac{1}{n} \sin n\theta \sin n\phi + 2\lambda(1-\bar{G}) \sum_{n=1}^{\infty} \frac{V_f^n}{1+\bar{G}-(1-\bar{G})V_f^n} \frac{1}{n} \sin n\theta \sin n\phi \tag{47}$$

$$K_2(\theta, \phi) = (1+\lambda) \sum_{n=1}^{\infty} \frac{1}{n} \cos n\theta \cos n\phi + 2\lambda(1-\bar{G}) \sum_{n=1}^{\infty} \frac{V_f^n}{1+\bar{G}-(1-\bar{G})V_f^n} \frac{1}{n} \cos n\theta \cos n\phi. \tag{48}$$

Since $V_f < 1$, the second series in (47) and (48) are bounded while the first ones can be summed exactly to yield

$$\sum_{n=1}^{\infty} \frac{1}{n} \sin n\theta \sin n\phi = \frac{1}{2}\log\left|\sin\frac{\theta+\phi}{2}\right| - \frac{1}{2}\log\left|\sin\frac{\theta-\phi}{2}\right| \tag{49}$$

$$\sum_{n=1}^{\infty} \frac{1}{n} \cos n\theta \cos n\phi = -\frac{1}{2}\log\left|2\sin\frac{\theta+\phi}{2}\right| - \frac{1}{2}\log\left|2\sin\frac{\theta-\phi}{2}\right|. \tag{50}$$

Hence (49) and (50) show that the kernel functions become logarithmically singular at $\theta = \phi$. Note that the functions $f_s(\theta)$ $(s = 1, 2)$ on the right-hand-sides of (40) and (41) are well-behaved, and consequently the solutions to the integral equations (40) and (41), which possess logarithmically singular kernels, have a square-root singularity at $\theta = \alpha$ (Tuck, 1980).

Using (49) and (50), we write (40) and (41) as follows:

$$\int_{\alpha}^{\pi} \bar{H}_1(\phi)\bar{K}_1(\theta, \phi)\,\mathrm{d}\phi = g_1(\theta) \tag{51}$$

$$\bar{A}_0^{(2)} + \int_{\alpha}^{\pi} \bar{H}_1(\phi)\bar{K}_2(\theta, \phi)\,\mathrm{d}\phi = g_2(\theta) \tag{52}$$

where $A_0^{(2)} = (1+\lambda)a(\tau_0, G_m)\sin\beta\bar{A}_0^{(2)}$, and

$$\bar{K}_1(\theta, \phi) = \log\left|\sin\frac{\theta+\phi}{2}\right| - \log\left|\sin\frac{\theta-\phi}{2}\right| + \frac{4\lambda(1-\bar{G})}{1+\lambda}\sum_{n=1}^{\infty}\frac{V_f^n}{1+\bar{G}-(1-\bar{G})V_f^n}\frac{1}{n}\sin n\theta \sin n\phi \tag{53}$$

$$\bar{K}_2(\theta, \phi) = -\log\left|2\sin\frac{\theta+\phi}{2}\right| - \log\left|2\sin\frac{\theta-\phi}{2}\right| + \frac{4\lambda(1-\bar{G})}{1+\lambda}\sum_{n=1}^{\infty}\frac{V_f^n}{1+\bar{G}-(1-\bar{G})V_f^n}\frac{1}{n}\cos n\theta \cos n\phi \tag{54}$$

$$g_1(\theta) = \frac{4}{(1+\lambda)[1+\bar{G}-(1-\bar{G})V_f]}\sin\theta \tag{55}$$

$$g_2(\theta) = \frac{4}{(1+\lambda)[1+\bar{G}-(1-\bar{G})V_f]}\cos\theta. \tag{56}$$

The coefficient $\bar{A}_0^{(2)}$ is determined by the auxiliary equation (42).

Hence the solution of the dual series equations (26)–(27) and (28)–(29) is reduced to the solution of the Fredholm integral equations (51) and (52).

CALCULATION OF THE EFFECTIVE MODULUS

By applying the average stress theorem, the average fiber stress in (5) can be written as

$$\bar{\tau}^{\mathrm{f}}_{23} = \frac{1}{A_{\mathrm{f}}}\int_{S_0+S_{\mathrm{c}}} T_3\bar{x}_2\,\mathrm{d}s \tag{57}$$

where A_{f} is the total cross area of all fibers, S_0 is the contour of all the interfaces without cracks and T_3 is the shear traction at the interfaces.

Let us assume that for simplicity all fibers have equal radius a. It follows that $A_{\mathrm{f}} = N_{\mathrm{f}}\pi a^2$, where N_{f} is the number of fibers. Following the procedure of the generalized self-consistent scheme, the integral over the uncracked interfaces can be easily calculated. The result is

$$\frac{1}{A_{\mathrm{f}}}\int_{S_0} T_3\bar{x}_2\,\mathrm{d}s = (1-n_{\mathrm{c}})\frac{4\lambda}{(\lambda+1)(1+\bar{G})+(\lambda-1)(1-\bar{G})V_{\mathrm{f}}}\tau_0 \tag{58}$$

where $n_{\mathrm{c}} = N_{\mathrm{c}}/N_{\mathrm{f}}$ is the interface crack number fraction, N_{c} being the number of fibers that contain interface cracks. In terms of the local polar coordinates we have from (57) and (58)

$$\bar{\tau}^{\mathrm{f}}_{23} = (1-n_{\mathrm{c}})\frac{4\lambda}{(\lambda+1)(1+\bar{G})+(\lambda-1)(1-\bar{G})V_{\mathrm{f}}}\tau_0 + \frac{n_{\mathrm{c}}}{\pi}\frac{1}{N_{\mathrm{c}}}\sum_{\alpha,\beta}\int_{-\pi}^{\pi} T_3(\theta;\alpha,\beta)\sin(\theta+\beta)\,\mathrm{d}\theta \tag{59}$$

where the summation is taken over all possible values of α and β.

Since $T_3(\theta) = H_1(\theta)+H_2(\theta)$ for $\alpha \leqslant \theta \leqslant \pi$, $-\pi \leqslant \theta \leqslant -\alpha$ where $H_1(-\theta) = -H_1(\theta)$, $H_2(-\theta) = H_2(\theta)$, and $T_3(\theta) = 0$ for $-\alpha \leqslant \theta \leqslant \alpha$, it follows that

$$\frac{\bar{\tau}^{\mathrm{f}}_{23}}{\tau_0} = (1-n_{\mathrm{c}})\frac{4\lambda}{(\lambda+1)(1+\bar{G})+(\lambda-1)(1-\bar{G})V_{\mathrm{f}}} + 2\lambda n_{\mathrm{c}}\frac{1}{N_{\mathrm{c}}}\sum_{\alpha,\beta}\left\{\cos^2\beta\int_{\alpha}^{\pi}\bar{H}_1(\theta)\sin\theta\,\mathrm{d}\theta+\sin^2\beta\int_{\alpha}^{\pi}\bar{H}_2(\theta)\cos\theta\,\mathrm{d}\theta\right\}. \tag{60}$$

Notice that as before we do not write the explicit dependence of $H_s(\theta)$ or $\bar{H}_s(\theta)$ $(s = 1, 2)$ on α. For convenience we will continue to do so when there is no danger of confusion.

As discussed earlier, we postulate that the interface cracks are randomly located so that the angle β varies from 0 to 2π. In addition, we introduce a distribution function $f(\alpha)$ such that the fraction of cracks whose half crack lengths have values between c and $c+\mathrm{d}c$ where $c = \alpha a$ is given by $f(\alpha)\,\mathrm{d}\alpha$. Thus, the summation in (60) can be replaced by an integration as follows:

$$\frac{\bar{\tau}^{\mathrm{f}}_{23}}{\tau_0} = (1-n_{\mathrm{c}})\frac{4\lambda}{(\lambda+1)(1+\bar{G})+(\lambda-1)(1-\bar{G})V_{\mathrm{f}}} + 2n_{\mathrm{c}}\lambda\int_{\alpha_1}^{\alpha_2} f(\alpha)\,\mathrm{d}\alpha \times\left\{\left[\frac{1}{2\pi}\int_0^{2\pi}\cos^2\beta\,\mathrm{d}\beta\right]\int_{\alpha}^{\pi}\bar{H}_1(\theta)\sin\theta\,\mathrm{d}\theta+\left[\frac{1}{2\pi}\int_0^{2\pi}\sin^2\beta\,\mathrm{d}\beta\right]\int_{\alpha}^{\pi}\bar{H}_2(\theta)\cos\theta\,\mathrm{d}\theta\right\} \tag{61}$$

where $\alpha_1 a \leqslant c \leqslant \alpha_2 a$ gives the range of the interface crack length.

Hence we have

$$\frac{\bar{\tau}^{\mathrm{f}}_{23}}{\tau_0} = (1-n_{\mathrm{c}})\frac{4\lambda}{(\lambda+1)(1+\bar{G})+(\lambda-1)(1-\bar{G})V_{\mathrm{f}}} + n_{\mathrm{c}}\lambda\int_{\alpha_1}^{\alpha_2} f(\alpha)\,\mathrm{d}\alpha\left\{\int_{\alpha}^{\pi}\bar{H}_1(\theta)\sin\theta\,\mathrm{d}\theta+\int_{\alpha}^{\pi}\bar{H}_2(\theta)\cos\theta\,\mathrm{d}\theta\right\}. \tag{62}$$

In the local polar coordinates, by using the fact that $V_f = N_f\pi a^2/A$ the integral of displacement jump at the cracked interfaces Γ_{23} in (3) can be written in the form

$$\Gamma_{23} = \frac{V_f n_c}{\pi a}\frac{1}{N_c}\sum_{\alpha,\beta}\int_{-\alpha}^{\alpha}[w]\sin(\theta+\beta)\,d\theta \tag{63}$$

where $[w] = w^m(a,\theta) - w^f(a,\theta)$. It can be shown that the following expression is true:

$$[w] = \frac{4}{1+\bar{G}-(1-\bar{G})V_f}\frac{\tau_0}{G_m}a\sin(\theta+\beta)$$
$$-A_0^{(2)} - \sum_{n=1}^{\infty} a^n(1+\beta_n)(A_n^{(1)}\sin n\theta + A_n^{(2)}\cos n\theta). \tag{64}$$

Inserting (64) into (63), using (37) and (38), and after some manipulation we obtain the following result:

$$\frac{G_m}{\tau_0}\Gamma_{23} = \frac{V_f n_c}{\pi}\frac{1}{N_c}\sum_{\alpha,\beta}\left\{-2(1+\lambda)\sin^2\beta\sin\alpha\bar{A}_0^{(2)} + \frac{4}{1+\bar{G}-(1-\bar{G})V_f}\right.$$
$$\times[\alpha+\tfrac{1}{2}\sin 2\alpha(\sin^2\beta-\cos^2\beta)] - 4\cos^2\beta\int_0^{\alpha}\int_{\alpha}^{\pi}\bar{H}_1(\phi)K_1(\theta,\phi)\sin\theta\,d\theta\,d\phi$$
$$\left.-4\sin^2\beta\int_0^{\alpha}\int_{\alpha}^{\pi}\bar{H}_2(\theta)K_2(\theta,\phi)\cos\theta\,d\theta\,d\phi\right\}. \tag{65}$$

As discussed before the summation in (65) can be replaced by an integration through the aforementioned distribution function $f(\alpha)$. After carrying out the integration with respect to β, we obtain

$$\frac{G_m}{\tau_0}\Gamma_{23} = \frac{V_f n_c}{\pi}\int_{\alpha_1}^{\alpha_2} f(\alpha)\,d\alpha\left\{-(1+\lambda)\sin\alpha\bar{A}_0^{(2)} + \frac{4}{1+\bar{G}-(1-\bar{G})V_f}\alpha\right.$$
$$\left.-2\int_0^{\alpha}\int_{\alpha}^{\pi}\bar{H}_1(\phi)K_1(\theta,\phi)\sin\theta\,d\theta\,d\phi - 2\int_0^{\alpha}\int_{\alpha}^{\pi}\bar{H}_2(\phi)K_2(\theta,\phi)\cos\theta\,d\theta\,d\phi\right\}. \tag{66}$$

Thus the effective longitudinal shear modulus is calculated via the solution of the equation

$$\bar{G}^{-1} = 1 + V_f\left(\frac{1}{\lambda}-1\right)\frac{\bar{\tau}_{23}^f}{\tau_0} + \frac{G_m}{\tau_0}\Gamma_{23}. \tag{67}$$

NUMERICAL SOLUTIONS AND RESULTS

It is well known that in general a Fredhom integral equation of the first kind can be very difficult to solve numerically. Indeed this fact might partly account for the past preference for reducing dual series equations to an integral equation of the second kind (Westman and Yang, 1967; Keer and Sve, 1970; Keer *et al.*, 1973). An effective technique for numerically solving singular integral equations of the first kind with a dominant Cauchy type singularity, which are frequently encountered in fracture mechanics analysis, has been proposed by Erdogan and Gupta (1972), but no general numerical treatment of the type of the integral equation under present consideration appears to exist in the literature. Nonetheless, the logarithmic singularity present in the current problem makes the integral equations (51) and (52) suitable for a numerical solution that will be described here.

First note that the solutions contain the square-root singularity at the end point $\phi = \alpha$. To incorporate such singularity in the solutions, we introduce bounded functions $h_s(\phi)$, $s = 1, 2$, such that

$$\bar{H}_s(\phi) = \frac{h_s(\phi)}{\sqrt{\phi-\alpha}}, \quad \alpha \leqslant \phi \leqslant \pi. \tag{68}$$

To solve the integral equations (51) and (52) in combination with (42) we divide the interval $[\alpha, \pi]$ into N subintervals $[\phi_{j-1}, \phi_j]$, $j = 1, 2, \ldots, N$ and by substituting (68) into (51), (52) and auxiliary equation (42), we have

$$\sum_{j=1}^{N} \int_{\phi_{j-1}}^{\phi_j} \bar{K}_1(\theta, \phi) \frac{h_1(\phi)}{\sqrt{\phi-\alpha}} \, d\phi = g_1(\theta) \tag{69}$$

$$\bar{A}_0^{(2)} + \sum_{j=1}^{N} \int_{\phi_{j-1}}^{\phi_j} \bar{K}_2(\theta, \phi) \frac{h_2(\phi)}{\sqrt{\phi-\alpha}} \, d\phi = g_2(\theta) \tag{70}$$

$$\sum_{j=1}^{N} \int_{\phi_{j-1}}^{\phi_j} \frac{h_2(\phi)}{\sqrt{\phi-\alpha}} \, d\phi = 0. \tag{71}$$

Then we approximate $h_s(\phi)$ by a step function, i.e. replace it within the jth subinterval $[\phi_{j-1}, \phi_j]$ by a constant $h_j^{(s)}$ ($s = 1, 2$), which gives

$$\sum_{j=1}^{N} h_j^{(1)} \int_{\phi_{j-1}}^{\phi_j} \frac{\bar{K}_1(\theta, \phi)}{\sqrt{\phi-\alpha}} \, d\phi \approx g_1(\theta) \tag{72}$$

$$\bar{A}_0^{(2)} + \sum_{j=1}^{N} h_j^{(2)} \int_{\phi_{j-1}}^{\phi_j} \frac{\bar{K}_2(\theta, \phi)}{\sqrt{\phi-\alpha}} \, d\phi \approx g_2(\theta) \tag{73}$$

$$\sum_{j=1}^{N} h_j^{(2)} \int_{\phi_{j-1}}^{\phi_j} \frac{1}{\sqrt{\phi-\alpha}} \, d\phi \approx 0. \tag{74}$$

If we now evaluate the integrals in (72) and (73) at the mid-point of each subinterval and carry out the integration in (74) we arrive at the following systems of linear equations

$$\sum_{j=1}^{N} \bar{K}_{ij}^{(1)} h_j^{(1)} = g_i^{(1)} \tag{75}$$

$$\bar{A}_0^{(2)} + \sum_{j=1}^{N} \bar{K}_{ij}^{(2)} h_j^{(2)} = g_i^{(2)} \tag{76}$$

$$\sum_{j=1}^{N} K_j h_j^{(2)} = 0 \tag{77}$$

$$i = 1, 2, \ldots, N$$

where

$$\bar{K}_{ij}^{(s)} = \int_{\phi_{j-1}}^{\phi_j} \frac{\bar{K}_s(\theta_i, \phi)}{\sqrt{\phi-\alpha}} \, d\phi \tag{78}$$

$$K_j = 2(\sqrt{\phi_j-\alpha} - \sqrt{\phi_{j-1}-\alpha}) \tag{79}$$

$$g_i^{(s)} = g_s(\theta_i) \tag{80}$$

$$\theta_i = \tfrac{1}{2}(\phi_{i-1}+\phi_i) \tag{81}$$

$$s = 1, 2.$$

A modified version of the so-called Chebyshev mesh is used, giving

$$\phi_j = \pi-(\pi-\alpha)\cos\frac{j\pi}{2N}, \quad j = 0, 1, 2, \ldots N. \tag{82}$$

It has the feature of allocating more mesh points near the crack tip $\phi = \alpha$, which is obviously desirable in view of the expected stress singularity there.

The functions $\bar{K}_s(\theta_i, \phi)$ in (78) become unbounded at $\phi = \theta_i$, thus conventional quadrature formulae will not yield sufficient accuracy. To circumvent such difficulty, we write the kernels (53) and (54) in the following manner

$$\bar{K}_s(\theta, \phi) = \bar{K}_0^{(s)}(\theta, \phi)+\bar{K}_1^{(s)}(\theta, \phi) \tag{83}$$

$$s = 1, 2$$

where

$$\bar{K}_0^{(1)}(\theta, \phi) = \log\left|\frac{\theta+\phi}{\theta-\phi}\right|+\log|2\pi-\theta-\phi| \tag{84}$$

$$\bar{K}_1^{(1)}(\theta, \phi) = \log\left|\frac{\sin(\theta+\phi)/2}{(2\pi-\theta-\phi)(\theta+\phi)/2}\right|-\log\left|\frac{\sin(\theta-\phi)/2}{(\theta-\phi)/2}\right| + \frac{4\lambda(1-\bar{G})}{1+\lambda}\sum_{n=1}^{\infty}\frac{V_1^n}{1+\bar{G}-(1-\bar{G})V_1^n}\frac{1}{n}\sin n\theta\sin n\phi \tag{85}$$

$$\bar{K}_0^{(2)}(\theta, \phi) = -\log|\theta+\phi|-\log|\theta-\phi|-\log|2\pi-\theta-\phi| \tag{86}$$

$$\bar{K}_1^{(2)}(\theta, \phi) = -\log\left|\frac{\sin(\theta+\phi)/2}{(2\pi-\theta-\phi)(\theta+\phi)/2}\right|-\log\left|\frac{\sin(\theta-\phi)/2}{(\theta-\phi)/2}\right| + \frac{4\lambda(1-\bar{G})}{1+\lambda}\sum_{n=1}^{\infty}\frac{V_1^n}{1+\bar{G}-(1-\bar{G})V_1^n}\frac{1}{n}\cos n\theta\cos n\phi. \tag{87}$$

It follows that

$$\bar{K}_{ij}^{(s)} = \int_{\phi_{j-1}}^{\phi_j}\frac{\bar{K}_0^{(s)}(\theta_i, \phi)}{\sqrt{\phi-\alpha}}\,d\phi+\int_{\phi_{j-1}}^{\phi_j}\frac{\bar{K}_1^{(s)}(\theta_i, \phi)}{\sqrt{\phi-\alpha}}\,d\phi \tag{88}$$

$$s = 1, 2; \quad j = 1, 2, \ldots, N.$$

The first integrals in (88) can be integrated exactly and since $K_1^{(s)}(\theta, \phi)$ is well behaved, through a change of variable $u = \sqrt{\phi-\alpha}$, the second integrals may be calculated by any numerical method, for instance, Simpson's rule is found to be quite effective.

For the purpose of illustration, in the subsequent numerical calculations we consider a simple situation when the interface crack length is uniformly distributed between 0 and $2\pi a$ with the distribution function given by

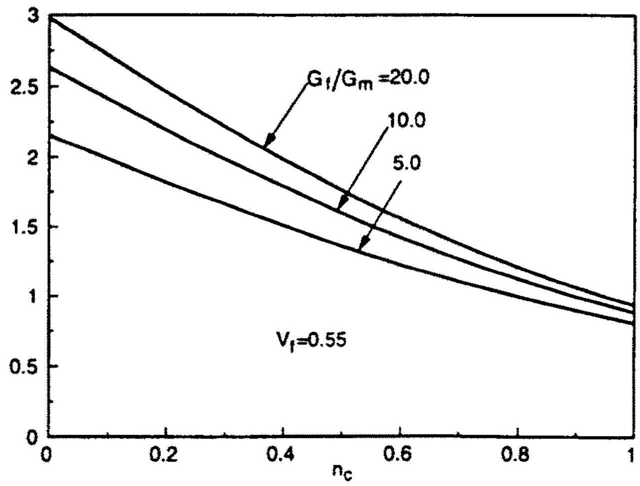

Fig. 4. Effective longitudinal shear modulus vs fraction of fibers containing interface cracks. $V_f = 0.55$.

$$f(\alpha) = \frac{1}{\pi}, \quad 0 < \alpha < \pi. \tag{89}$$

Calculations of the effective shear modulus were carried out for various interface crack number fractions, ratios of fiber-matrix moduli and fiber volume contents. The bisection method was found to be quite effective in solving eqn (67) for G_e. The results are presented in Figs 4–8.

Figure 4 shows the variation of G_e with interface crack number fraction n_c for various ratios G_f/G_m. The results indicate that the rate of reduction in longitudinal shear stiffness increases with the increase of G_f/G_m. Figures 5–6 show the variation of G_e with interface crack number fraction for various values of V_f. Note that for a given n_c, the absolute number of fibers that contain interface cracks increases with the increase of fiber volume fraction. Figures 7–8 show the variation of G_e with fiber volume fraction for various n_c. The results presented in Figs 4–8 indicate that in the case when all fibers contain interface cracks, i.e. $n_c = 1$, the composite loses all the longitudinal stiffness reinforcement provided by the fibers. In interpreting these results, one should notice that in general, the number of interfacial cracks in the composite may well depend on the level of applied load as well as fiber volume content, and the crack length is likely to obey more complicated distribution

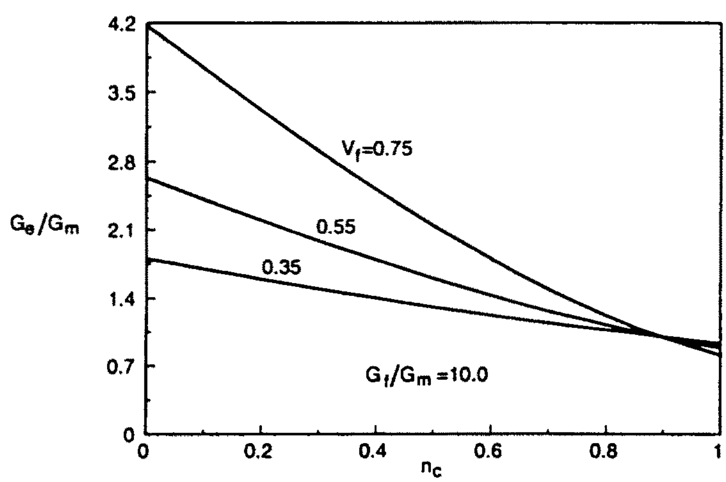

Fig. 5. Effective longitudinal shear modulus vs fraction of fibers containing interface cracks. $G_f/G_m = 10.0$.

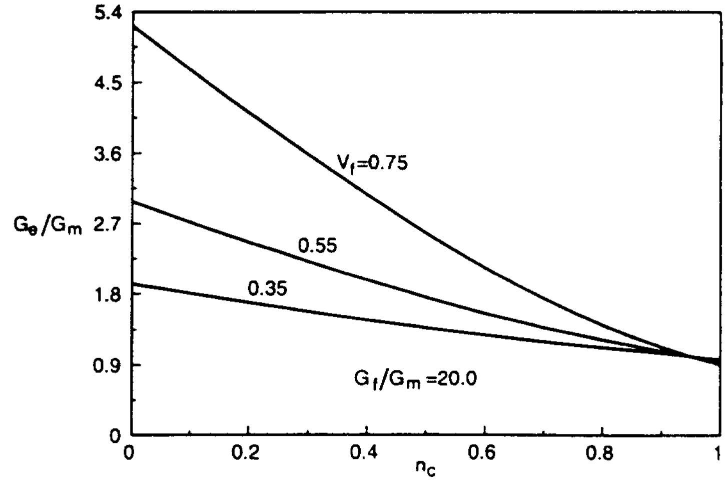

Fig. 6. Effective longitudinal shear modulus vs fraction of fibers containing interface cracks, $G_f/G_m = 20.0$.

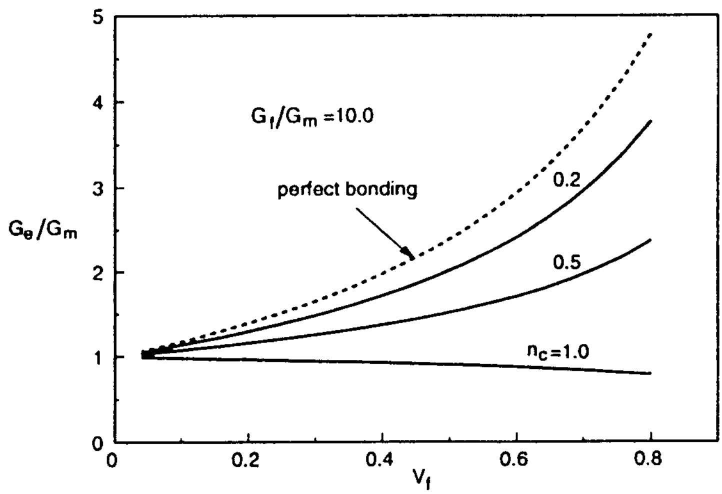

Fig. 7. Effective longitudinal shear modulus vs fiber volume fraction, $G_f/G_m = 10.0$.

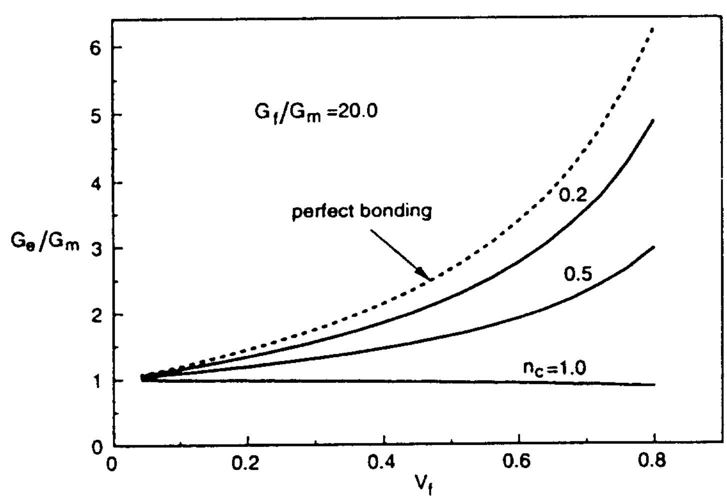

Fig. 8. Effective longitudinal shear modulus vs fiber volume fraction, $G_f/G_m = 20.0$.

functions (e.g., Gaussian distribution) than the simple uniform distribution function used here for numerical examples.

REFERENCES

Adams, D. F. and Doner, R. (1967). Longitudinal shear loading of a unidirectional composite. *J. Comp. Mater.* **1**, 4–17.

Budiansky, B. and Carrier, G. F. (1984). High stresses in stiff-fiber composites. *J. Appl. Mech.* **51**, 733–735.

Christensen, R. M. and Lo, K. H. (1979). Solutions for effective shear properties of three-phase sphere and cylinder models. *J. Mech. Phys. Solids* **27**, 315–330.

Comninou, M. (1990). An overview of interface cracks. *Engng Fract. Mech.* **37**, 197–208.

Delameter, W. R., Herrmann, G. and Barnett, D. M. (1975). Weakening of an elastic solid by a rectangular array of cracks. *J. Appl. Mech.* **42**, 74–80.

Erdogan, F. and Cupta, G. D. (1972). On numerical solution of singular integral equations. *Q. Appl. Math.* **30**, 533–547.

Hashin, Z. (1990). Thermoelastic properties of fiber composites with imperfect interface. *Mech. Mater.* **8**, 333–348.

Hoenig, A. (1979). Elastic moduli of non-randomly cracked body. *Int. J. Solids Structures* **15**, 137–154.

Keer, L. M., Dundurs, J. and Kiattikomol, K. (1973). Separation of a smooth inclusion from a matrix. *Int. J. Engng Sci.* **11**, 1221–1233.

Keer, L. M. and Sve, C. (1970). On the bending of cracked plates. *Int. J. Solids Structures* **6**, 1545–1559.

Laws, N., Dvorak, G. J. and Hejazi, M. (1983). Stiffness changes in unidirectional composites caused by crack systems. *Mech. Mater.* **2**, 123–137.

Steif, P. S. (1984). Stiffness reduction due to fiber breakage. *J. Comp. Mater.* **18**, 153–172.

Steif, P. S. and Dollar, A. (1988). Longitudinal shearing of a weakly bonded fiber composite. *J. Appl. Mech.* **55**, 618–623.

Takao, Y., Taya, M. and Chou, T. W. (1982). Effects of fiber-end cracks on the stiffness of aligned short-fiber composites. *Int. J. Solids Structures* **18**, 723–728.

Tuck, O. E. (1980). Application and solution of cauchy integral equations. In *The Application and Numerical Solution of Integral Equations* (Edited by R. S. Anderssen, F. R. de Hoog and M. A. Lukas), pp. 21–49. Sijthoff & Noordhoff, Alphen aan den Rijn, The Netherlands.

Westmann, R. A. and Yang, W. H. (1967). Stress analysis of cracked rectangular beams. *J. Appl. Mech.* **34**, 693–701.